High precision Mg isotope measurements of meteoritic samples by secondary ion mass spectrometry

Tu-Han Luu, Marc Chaussidon, Ritesh Kumar Mishra, Claire Rollion-Bard, Johan Villeneuve, Gopala Srinivasan, Jean-Louis Birck

HIGH PRECISION MG ISOTOPE MEASUREMENTS OF METEORITIC SAMPLES BY SECONDARY ION MASS SPECTROMETRY

Tu-Han Luu[a,b*], Marc Chaussidon[a], Ritesh Kumar Mishra[a], Claire Rollion-Bard[a], Johan Villeneuve[c], Gopalan Srinivasan[d] and Jean-Louis Birck[b]

[a] Centre de Recherches Pétrographiques et Géochimiques (CRPG) - INSU CNRS - Université de Lorraine - UPR 2300, 15 Rue Notre-Dame des Pauvres, BP20, 54501 Vandoeuvre-lès-Nancy Cedex, France.

[b] Laboratoire de Géochimie et Cosmochimie, Institut de Physique du Globe de Paris (IPGP), Sorbonne Paris Cité, 1 rue Jussieu, 75238 Paris Cedex 05, France.

[c] Institut des Sciences de la Terre d'Orléans - UMR 6113 - CNRS/Université d'Orléans, 1A rue de la Férollerie, 45071 Orléans Cedex 2, France.

[d] Center for Earth Sciences, Indian Institute of Science, Bangalore 560012, India.

* Corresponding author: luu@crpg.cnrs-nancy.fr

Keywords: Mg-isotope analyses, MC-SIMS, data reduction process, early solar system chronology, short-lived ^{26}Al.

Abstract

The possibility of establishing an accurate relative chronology of early solar system events based on the decay of short-lived ^{26}Al to ^{26}Mg (half-life of 0.72 Myr) depends on the level of homogeneity (or heterogeneity) of ^{26}Al and Mg isotopes. However this level is difficult to constrain precisely because of the very high precision needed on the determination of isotopic ratios, typically of ± 5 ppm. In this study, we report for the first time a very detailed analytical protocol developed for high precision *in situ* Mg isotopic measurements (^{25}Mg/^{24}Mg and ^{26}Mg/^{24}Mg ratios, as well as ^{26}Mg excess) by MC-SIMS. As the data reduction process is critical for both accuracy and precision of the final isotopic results, factors such as the Faraday cup (FC) background drift and matrix effects on instrumental fractionation have been investigated. Indeed these instrumental effects impacting the measured Mg-isotope ratios can be as large or larger than the variations we are looking for to

constrain the initial distribution of ^{26}Al and Mg isotopes in the early solar system. Our results show that they definitely are limiting factors regarding the precision of Mg isotopic compositions, and that an under- or over-correction of both FC background instabilities and instrumental isotopic fractionation leads to important bias on $\delta^{25}Mg$, $\delta^{26}Mg$ and $\Delta^{26}Mg$ values (for example, olivines not corrected for FC background drifts display $\Delta^{26}Mg$ values that can differ by as much as 10 ppm from the truly corrected value). The new data reduction process described here can then be applied to meteoritic samples (components of chondritic meteorites for instance) to accurately establish their relative chronology of formation (actually the time of their isotopic closure).

1 Introduction

Variations of the Mg isotopic composition of meteoritic materials can be understood at first order to be the sum of (i) mass-dependent isotopic fractionations due to processes such as evaporation or condensation, and (ii) decay of short-lived ^{26}Al to ^{26}Mg (half-life of 0.72 Myr). Calcium-, aluminum-rich inclusions (CAIs), that are the oldest dated solids formed in the accretion disk around the early sun,[1-3] display large ^{26}Mg excesses.[4] They can be used to define the initial $^{26}Al/^{27}Al$ ratio ($5.23(\pm0.13)\times10^{-5}$,[5,6]) that anchors the ^{26}Al-based chronology. However, the ^{26}Al-^{26}Mg system can be used as a chronometer only under the assumption that ^{26}Al and Mg isotopes were homogenized early in the accretion disk.

The level of homogeneity (or heterogeneity) is difficult to constrain precisely. One way is to be able to compare ^{26}Mg excesses measured with high precision in samples formed at various ages in the accretion disk with ^{26}Mg excesses predicted assuming homogeneity. For a solar $^{27}Al/^{24}Mg$ ratio of 0.101,[7] (this ratio being estimated from CI chondrites, and not the solar photosphere) ^{26}Mg produced from the total decay of an initial $^{26}Al/^{27}Al$ ratio of 5.23×10^{-5} increases the $^{26}Mg/^{24}Mg$ ratio by ~ 38 ppm. The magnitude of the ^{26}Mg excesses measured *in situ* by MC-SIMS (multi-collection secondary ion mass spectrometry) in ferromagnesian chondrules (chondrules are mm-sized objects which were melted and quenched in the accretion disk and they constitute the major high-temperature component of primitive meteorites) from ordinary chondrites does support a ± 10% homogeneous distribution of ^{26}Al and Mg isotopes at the time of CAI formation in the disk.[8] This view has been challenged[9] from very high precision bulk analyses (± 2.5 ppm for ^{26}Mg excesses[10]) of refractory components of carbonaceous chondrites (CAIs and amoeboid olivine aggregates) by HR-MC-

ICPMS (high-resolution multi-collector inductively coupled plasma source mass spectrometry).

One key to the debate is the development of high precision for Mg isotopic measurements, both bulk and *in situ*. In fact, the studied objects (i.e. CAIs) underwent, after their formation from precursors condensed from the gas, several high temperature events including melting and re-crystallization. If melting/crystallization occurred in closed system, it did not modify the bulk compositions (Mg and Al isotopes and Al/Mg ratio) so that a bulk ^{26}Al isochron gives theoretically access to the Al and Mg isotopic compositions of the precursors and thus dates condensation. At variance *in situ* analysis by MC-SIMS allows to look for the existence of a ^{26}Al mineral isochron within one object, which would date the partitioning of Al and Mg between the different constituent minerals during the last melting/crystallization event. The combination of bulk and *in situ* data should allow to reconstruct the history of the high temperature components of meteorites, from early condensation events to late melting or re-melting processes.

A high precision Mg isotopic measurements method has already been developed for HR-MC-ICPMS.[10] However bulk analyses by HR-MC-ICPMS require a large sample size and do not allow to determine mineral isochrons because of the high spatial resolution required in the case of early solar system objects.

Here we describe the analytical protocol developed for high precision Mg isotopic measurements (^{25}Mg/^{24}Mg and ^{26}Mg/^{24}Mg ratios, as well as ^{26}Mg excess) of meteoritic samples by MC-SIMS on ~ 30-40 μm analytical spots. This protocol is a further refinement of that developed by Villeneuve *et al.*[8,11]. Other groups are developing these measurements[12-15] but their procedure is not yet described in full detail. The factors limiting the precision are assessed. An example of application to the study of several components of chondritic meteorites is given.

2 Data acquisition

Mg-isotope ratios and Al/Mg ratios are measured using the CRPG-CNRS (Nancy) CAMECA large radius ims 1270 and ims 1280HR2 ion microprobes (some instrument configuration and capabilities of MC-SIMS can be found in Benninghoven *et al.*[16] and De Chambost[17]). Gold coated or carbon coated polished thick sections of samples are sputtered by a 13 kV O^- static primary beam and positive secondary ions of Al and Mg isotopes are

extracted and accelerated at 10 kV. The intensity of the primary beam is set to produce the highest possible count rate for secondary ions (i.e. > 1×10^9 counts per second (cps) on $^{24}Mg^+$, in olivines), while keeping the beam diameter small enough to allow the analysis of individual mineral phases in chondrules or CAIs: for instance a ~ 30 nA primary beam intensity corresponds to a ~ 30-40 μm spot size. The secondary ions are analyzed at a mass resolution M/ΔM = 2500 (using exit slit #1 of the multicollector) in multicollection mode using four Faraday cups (FCs): L'2, C, H1 and H'2, for ^{24}Mg, ^{25}Mg, ^{26}Mg and ^{27}Al, respectively. Such a low mass resolution is chosen to maximize the flatness of the three Mg peaks though the interference of the hydride $^{24}MgH^+$ on ^{25}Mg (with a vacuum in the sample chamber below 3×10^{-9} torr, the contribution of $^{24}MgH^+$ on ^{25}Mg is less than 10^{-6} relative) is not totally resolved (a M/ΔM of 3559 would be required). However measurements made at higher mass resolution (M/ΔM = 6000 using exit slit #2) have shown that the contribution of the hydride on ^{25}Mg remains < a few cps, i.e. < ~10^{-8} relative for ^{25}Mg (whose intensity is > a few 10^8 cps in olivines) if the vacuum in the chamber is < 3×10^{-9} torr.

Each analysis of a new sample mount starts by a manual setting of the Z position of the mount to keep constant the distance between the sample surface and the front plate of the immersion lens. When possible, different grains of different international and in-house standards are included with the sample(s) to analyze in the same mount. In addition, different mounts containing standards are also analyzed in between mounts containing samples and standards. Generally, analyses are automatically chained. A chain of analyses can include both depth profiles (in that case no more than 7 measurements are done at the same spot) and analyses at different spots on a same grain or on different grains (standard or sample) close to each other in the mount (in that case the sample stage is moved, only over a short distance, but allowing much more analyses to be done, the number depending on the spot size). Whatever the case the primary beam never moves. One typical analysis lasts 425 s, including a total of 150 s presputtering and 275 s simultaneous counting of the intensities of $^{24}Mg^+$, $^{25}Mg^+$, $^{26}Mg^+$ and $^{27}Al^+$ (25 cycles of 10 s counting time separated by 1 s waiting time). During presputtering, the background of each FC is measured (the secondary beam is deflected from the entrance of the magnet by the deflector Y of the coupling lens LC1C) and an automatic centering of the secondary beam is performed (using secondary intensity measured for ^{24}Mg) either in the field aperture (using transfer lenses deflectors LTdefxy) with the ims 1270 or in both the field aperture and the contrast aperture (using transfer lenses deflectors DTFAxy and DTCAxy) with the ims 1280HR2. This automatic centering allows

correction of the secondary beam trajectory for possible small deviations due to imperfect alignment or flatness of the sample. In addition to these centerings, the charging of the sample is automatically monitored (and the secondary high voltage readjusted of a few volts if necessary) by scanning the energy distribution of secondary ions. The nuclear magnetic resonance (NMR) field sensor is used on the ims 1280HR2 to control and stabilize the magnetic field since no peak jumping is required because of the use of multi-collection.

2 Data reduction

At the level of precision required for Mg isotope analysis of extraterrestrial materials (e.g. 10 ppm or better on ^{26}Mg excesses noted Δ^{26}Mg, see section 3.5 for definition) the procedure of data reduction is critical to avoid introducing any analytical bias in the final isotopic results. This is particularly critical for MC-SIMS analysis for two major reasons. First, in MC-SIMS all measurements are direct measurements of isotopic compositions while in HR-MC-ICPMS, thanks to the standard-sample bracketing technique which cannot be used for SIMS, only differences of isotopic compositions are measured, thus eliminating most of the instrumental isotopic fractionations. Second, significant matrix effects are present and have a major influence on instrumental fractionation. However MC-SIMS has the advantage of a much lower instrumental fractionation, one order of magnitude less, than HR-MC-ICPMS. The approach developed to calibrate precisely and to correct for instrumental fractionation is described in the following, as well as the propagation of errors due to these different corrections.

In the following, Mg isotopic compositions will be expressed either as isotopic ratios or as delta values. The $\delta^{25,26}$Mg notation is the relative deviation, in per mil (‰), of the ^{25,26}Mg/^{24}Mg ratio from a reference isotopic composition (noted $(\delta^{x}\mathrm{Mg})_{\mathrm{DSM\ 3}}$ when the DSM 3 international standard is used).

$$(\delta^{x}Mg)_{DSM\,3} = \left[\frac{\left(\frac{^{x}Mg}{^{24}Mg}\right)_{sample}}{\left(\frac{^{x}Mg}{^{24}Mg}\right)_{DSM\,3}} - 1\right] \times 1000\,, \text{ where x stands for 25 or 26.}$$

The reference isotopic composition used to calculate the raw Mg-isotope ratios is that of SRM 980, with ^{25}Mg/^{24}Mg = 0.12663 and ^{26}Mg/^{24}Mg = 0.13932,[18] because the DSM 3 Mg-isotope ratios are determined relative to the SRM 980 international standard. A re-

evaluation of these ratios has recently been published ($^{25}Mg/^{24}Mg$ = 0.126896 and $^{26}Mg/^{24}Mg$ = 0.139652,[10]). However, as explained in the following, because most of the data reduction is made using isotopic ratios and not delta values, and because instrumental mass fractionation is calibrated from the analyses of different standards, the final corrected delta values are independent of the values taken as the reference isotopic ratios.

The capital delta notation ($\Delta^{26}Mg$, in ‰) will also be used hereafter to express ^{26}Mg excesses or deficits relative to a given mass fractionation law. In the case of a mass fractionation law for Mg isotopes characterized by a coefficient of 0.521, (see section 3.5 for more details), the $\Delta^{26}Mg$ value is calculated according to:

$$\Delta^{26}Mg = \delta^{26}Mg - \frac{\delta^{25}Mg}{0.521}.$$

Note that Ogliore et al.[19] have recently shown that in SIMS the mean of isotopic ratios determined from individual measurement cycles at low count rates is biased, yielding a long-run averaged ratio that is systematically higher than the true ratio. However, this effect is completely negligible at the high count rates used to measure the Mg-isotope ratios discussed in this paper.

3.1 Raw data and outlier rejection

The measured isotopic ratios averaged over 25 cycles and corrected only for the yields (determined from the Cameca calibration routine[20] at the beginning of each analytical session) and the backgrounds (determined during pre-sputtering) of the four Faraday cups are named raw data (e.g. $(^{25}Mg/^{24}Mg)_{raw}$). Several instrumental parameters are automatically registered with the raw data. Thus for each measurement raw data are accompanied by (i) the x and y sample positions (in μm) and a picture of the sample in reflected light through the ion probe microscope at the beginning of sputtering, (ii) the sample chamber pressure (in torr), (iii) the primary beam intensity (in A), (iv) the transfer deflectors values (LTdefxy for the ims 1270; DTFAxy and DTCAxy for the ims 1280HR2) which are automatically centered, (v) the drift of the secondary high voltage (in V) which is determined automatically, (vi) the background of the four FCs (in cps), (vii) the secondary intensities of $^{24}Mg^+$, $^{25}Mg^+$, $^{26}Mg^+$ and $^{27}Al^+$ (in cps), (viii) the $^{25}Mg/^{24}Mg$, $^{26}Mg/^{24}Mg$ and $^{26}Mg/^{25}Mg$ isotopic ratios, expressed in the $\delta^x Mg$ notation (with x = 25 or 26 for ratios to ^{24}Mg) with their associated 1 sigma error (1 s.e., n=25), a 2 standard deviation (2 s.d.) threshold being used to reject outliers within the 25 cycles (rejections of $\delta^{25}Mg$, $\delta^{26}Mg$ and $^{27}Al/^{24}Mg$ are independent so that rejected $\delta^{25}Mg$ and

δ^{26}Mg, if any, could correspond to different cycles), (ix) the $^{27}Al/^{24}Mg$ ratio and its associated 1 sigma error.

Results for which anomalies were observed during the analytical procedure are systematically discarded. They are identified from any of the following criteria: (i) secondary intensity normalized to primary beam intensity lower (by 20% or more) than the typical value observed on standards of similar matrix, (ii) spikes in the background measured for the FCs during pre-sputtering, (iii) anomalous charge (more than 15 V) of the sample (if any, it likely results from an incomplete charge compensation due to ageing of the mount metallization or its local removal when spots are close to each other), (iii) anomalously large re-centering of the transfer deflectors (in excess of ± 7 V), (iv) low statistic on either the δ^{25}Mg or δ^{26}Mg values (worse than 0.05‰, 1 s.e.). In addition, the samples are systematically observed after analyses with optical microscopy (or secondary electron microscopy) to discard analyses which would correspond to spots not entirely within a grain or spots touching a crack or an inclusion.

3.2 FC background drift

Significant drifts of FC backgrounds take place, primarily due to cyclic temperature variations (worst conditions for the air conditioning system result in an amplitude lower than ± 0.4°C over one day) in the ion probe room. As FC backgrounds are measured during the pre-sputtering at the beginning of each measurement, the raw $^{25}Mg/^{24}Mg$ and $^{26}Mg/^{24}Mg$ ratios are systematically corrected for background drift using a linear interpolation between two successive analyses. Note that the background variations of L'2, H1 and H'2 are correlated within each other, whereas they can be anti-correlated with the background variations of C.

If n_1 and n_2 are two count rates (in cps) for two Mg isotopes and Δb_1 and Δb_2 the drifts (in cps) estimated for their background variations from linear interpolation (Δ = measured background - extrapolated background), then the corrected n_1/n_2 isotope ratio writes:

$$\frac{n_1 + \Delta b_1}{n_2 + \Delta b_2} = \frac{n_1\left(1 + \frac{\Delta b_1}{n_1}\right)}{n_2\left(1 + \frac{\Delta b_2}{n_2}\right)} \approx \frac{n_1}{n_2} \times \left(1 + \frac{\Delta b_1}{n_1} - \frac{\Delta b_2}{n_2}\right),$$

It then comes that the per mil variations of the n_1/n_2 ratio can be expressed as:

$$\left[\left(\frac{\frac{n_1+\Delta b_1}{n_2+\Delta b_2}}{\frac{n_1}{n_2}}\right)-1\right]\times 1000=\left(\frac{\Delta b_1}{n_1}-\frac{\Delta b_2}{n_2}\right)\times 1000$$

So that finally, the delta values can be corrected for the background instabilities according to:

$$\left(\delta^x Mg\right)_{bkgcorr}=\left(\delta^x Mg\right)_{raw}+\frac{\Delta b_1}{n_1}\times 1000-\frac{\Delta b_2}{n_2}\times 1000, \text{ with x = 25 or 26.}$$

Two effects of this correction for drifts of background are significant (Fig. 1). Firstly, because the magnitude of the correction increases when count rates on the different Mg isotopes decrease, this correction will have a larger impact for Mg-poor minerals or glasses or in case of lower Mg secondary yield. This is the case for pyroxene and spinel relative to olivine. Secondly, because the count rates are about eight times lower on ^{25}Mg and ^{26}Mg relative to ^{24}Mg, the effect of the correction is non-mass dependent and impacts the magnitude of the ^{26}Mg excesses that can be calculated from the ^{25}Mg/^{24}Mg and ^{26}Mg/^{24}Mg ratios (with a maximum of 10 ppm change for olivines, Fig. 1).

3.3 Instrumental fractionation

Instrumental isotopic fractionation is produced in SIMS analysis during the extraction and acceleration of secondary ions from the sample, their analysis (transfer optic, electrostatic and magnetic sectors) in the mass spectrometer and their counting in the collectors of the multicollector. Instrumental fractionation resulting from differential breaking of chemical bonds in the sample depending on their vibration energies is a mass-dependent fractionation. Some phenomena which are minor contributors to the isotopic fractionation taking place in the spectrometer can be mass-independent, for example when improper tuning of the transfer optic results in the $^{24}Mg^+$, $^{25}Mg^+$ and $^{26}Mg^+$ ion beams not to be perfectly centered in the cross-over plane where they can be cut differently by the entrance slit of the spectrometer. In addition, improper tuning of the coupling optic (which refocuses the secondary beam between the electrostatic and magnetic sectors) may result in different off-axis aberrations of the secondary beam in the focal plane of the magnet (where the collectors are) and thus in slight differences of peak shapes for the three Mg isotopes and consequently some mass-independent fractionation. Because instrumental isotopic fractionation is primarily mass-dependent, it is generally named instrumental mass fractionation, but one important criteria of

proper tuning of the spectrometer is to minimize the mass-independent component of instrumental fractionation, which is indicated by the intercept in its calibration (see below).

Instrumental fractionation (α_{inst}) is defined for Mg isotopes as:

$$\alpha_{inst}^{x/24} = \left(\frac{^{x}Mg}{^{24}Mg}\right)_{bkgcorr} \Big/ \left(\frac{^{x}Mg}{^{24}Mg}\right)_{true}$$

where x stands for 25 or 26 and the subscripts *bkgcorr* and *true* stand for the ratio corrected for drifts of FC background and for the true isotope ratio, respectively. A set of terrestrial reference materials and international standards made of various mantle minerals (San Carlos olivine; Burma spinel; spinel, orthopyroxene and clinopyroxene from a peridotite xenolith from the Vitim volcanic field in Siberia[21]; orthopyroxene and clinopyroxene from pyroxenites BZCG (also known as BZ-37) and BZ-226, from Zabargad Island in the Red Sea[22]) and rocks (CLDR015V, BHVO and BCR2, three terrestrial basalt glasses), and of synthetic glasses (Bacati; glasses of anorthitic, pyroxenic and melilitic (Åk#70) compositions; two NIST SRM glasses[23]) is used to determine α_{inst} (Table 1). Because of the very small variation range of δ^{26}Mg in mantle rocks and high temperature minerals,[24] all standard mantle minerals are considered to have the same $^{26}Mg/^{24}Mg$ and $^{25}Mg/^{24}Mg$ ratios as San Carlos olivine ($\delta^{26}Mg_{DSM3}$ = -0.25(±0.04)‰ (2 s.d., n=29,[25]), $^{26}Mg/^{24}Mg$ = 0.1398284(±0.0000010), $^{25}Mg/^{24}Mg$ = 0.1268705(±0.0000005)), but measurements by MC-ICPMS are going on to check that for the few synthetic glasses.

Matrix effects on instrumental fractionation have been shown to follow a systematic often similar to that observed for natural isotopic fractionations between mineral or between minerals and fluids, as shown for example for D/H in amphiboles and micas.[26] By analogy with the exponential law ($\alpha_{inst}^{25/24} = (\alpha_{inst}^{26/24})^{\beta}$) generally used[27] to express Mg isotopic fractionations for terrestrial or meteoritic samples, the instrumental fractionation law is determined from a linear regression (with the Isoplot 3.00 software[28]) between $\ln(\alpha_{inst}^{25/24})$ and $\ln(\alpha_{inst}^{26/24})$ measured for the different international and in-house standards. The instrumental law is always of the following form:[29]

$$\ln(\alpha_{inst}^{26/24}) = \left[\ln(\alpha_{inst}^{25/24}) - b\right] \Big/ \beta_{inst}$$

with β_{inst} varying between 0.51075 and 0.52045 and the intercept b slightly different from 0 with values typically from -0.00058 to -0.00030. Values of β_{inst} and of b appear to vary independently between different analytical sessions. This instrumental law can be expressed as:

$$\alpha_{inst}^{25/24} = \exp(b) \times (\alpha_{inst}^{26/24})^{\beta_{inst}}$$

where it is clear that it differs slightly from a purely mass dependent law because of the term $\exp(b)$.

For b very close to 0, one can approximate the above equation by:

$$\alpha_{inst}^{25/24} \approx (\alpha_{inst}^{26/24})^{\beta_{inst}}$$

Large variations of $\alpha_{inst}^{25/24}$ due to matrix effects, i.e. caused by variations of vibrational energies of the bonds involving Mg isotopes in minerals or glasses having different chemical compositions, are present among silicates and oxides (Fig. 2). In the case of olivines for instance, a similar effect than previously reported for O isotopes[30] exists for Mg isotopes. Values of $\alpha_{inst}^{25/24}$ increase by ~ 1‰/amu from Fo#79 (olivine from the Eagle Station pallasite) to Fo#88 (San Carlos olivine), and this trend can be linearly extrapolated to determine $\alpha_{inst}^{25/24}$ for olivines with Fo# > 88. Similarly for melilite, a change of 1.9‰/amu is observed between two melilite glasses having different Al/Mg ratios. Matrix effects between silicates and oxides are of similar magnitude, e.g. ~ 2‰/amu between pyroxene and spinel.

When the instrumental fractionation law has been properly determined, the $(^{25}Mg/^{24}Mg)_{bkgcorr}$ ratio of a given sample is corrected for the appropriate value of $\alpha_{inst}^{25/24}$ determined from the calibration based on standards with different compositions. Then, the corresponding value of $\alpha_{inst}^{26/24}$ is calculated from the instrumental fractionation law (using the values determined for β_{inst} and b) and is used to correct the $(^{26}Mg/^{24}Mg)_{bkgcorr}$ ratio. The two Mg-isotope ratios obtained are considered as the "true isotopic ratios" of the sample, in the sense that they are corrected for all ion probe instrumental effects and seem the closest possible to the true values.

3.4 Determination of $(\delta^{25}Mg)_{DSM\,3}$ and $(\delta^{26}Mg)_{DSM\,3}$.

The $(\delta^{25}Mg)_{DSM\,3}$ and $(\delta^{26}Mg)_{DSM\,3}$ values are calculated from the $(^{25}Mg/^{24}Mg)_{true}$ and $(^{26}Mg/^{24}Mg)_{true}$ ratios respectively (see above), and are expressed with respect to the DSM 3 standard.

The 2 sigma error on the $\delta^{25}Mg$ value of an individual measurement $(2\sigma_{(\delta^{25}Mg)_{ind\text{-}meas}})$ is calculated as the quadratic sum of (i) the external reproducibility determined from repetitive

analyses of standards of same matrix than the sample ($2\sigma_{(\delta^{25}\mathrm{Mg})_{\mathrm{std}}}$) and (ii) the internal error due to the counting statistic ($2\sigma_{(\delta^{25}\mathrm{Mg})_{\mathrm{bkgcorr}}}$) according to:

$$2\sigma_{(\delta^{25}\mathrm{Mg})_{\mathrm{ind\text{-}meas}}} = \sqrt{(2\sigma_{(\delta^{25}\mathrm{Mg})_{\mathrm{std}}})^2 + (2\sigma_{(\delta^{25}\mathrm{Mg})_{\mathrm{bkgcorr}}})^2}\,.$$

The component which dominates by far in the error is the external reproducibility (typically not better than ± 0.150‰ for olivine for instance) which is one order of magnitude higher than counting statistic error (typically better than ± 0.021‰ for olivine for instance). The 2 sigma error on the δ^{26}Mg value of an individual measurement ($2\sigma_{(\delta^{26}\mathrm{Mg})_{\mathrm{ind\text{-}meas}}}$) is calculated similarly.

3.5 Calculation of ^{26}Mg excess or deficit and error propagation

The ^{26}Mg excesses or deficits, written in capital delta notation Δ^{26}Mg (in ‰), are calculated directly from the true isotopic ratios using the following relationship:

$$\Delta^{26}\mathrm{Mg} = \left[\left(\frac{^{26}\mathrm{Mg}}{^{24}\mathrm{Mg}} \right)_{true}^{sample} \Big/ \left[\left(\frac{^{26}\mathrm{Mg}}{^{24}\mathrm{Mg}} \right)_{DSM\,3} \times \left[\frac{\left(\frac{^{25}\mathrm{Mg}}{^{24}\mathrm{Mg}} \right)_{true}^{sample}}{\left(\frac{^{25}\mathrm{Mg}}{^{24}\mathrm{Mg}} \right)_{DSM\,3}} \right]^{1/\beta} \right] - 1 \right] \times 1000\,,$$

with $\beta = \beta_{\mathrm{Earth}}$ or β_{met} (see below), $(^{25}\mathrm{Mg}/^{24}\mathrm{Mg})_{DSM3} = 0.126887$, $(^{26}\mathrm{Mg}/^{24}\mathrm{Mg})_{DSM3} = 0.139863$. These ratios were calculated from $(\delta^{26}Mg)_{SRM\,980}^{DSM\,3}$ = 3.90(±0.03)‰ (2s.e.), $(\delta^{26}Mg)_{SRM\,980}^{DSM\,3}$ standing for the δ^{26}Mg of DSM 3, expressed with respect to the SRM 980 international standard.[31-32] However the isotopic homogeneity of the SRM 980 standard has been challenged.[33] Calculation with $(\delta^{26}Mg)_{SRM\,980}^{DSM\,3}$ = 3.40(±0.13)‰[33] result in a 0.007‰ decrease on Δ^{26}Mg values for extraterrestrial materials (that remains within the error bar of the Δ^{26}Mg value calculated with $(\delta^{26}Mg)_{SRM\,980}^{DSM\,3}$ = 3.9‰), whereas no change is seen for terrestrial materials. This is because the β value used to calculate Δ^{26}Mg values for terrestrial samples is 0.521 (β_{Earth}, corresponding to equilibrium Mg isotopic fractionations[34]), and 0.514 for meteoritic olivines (β_{met}).[35] This value of 0.514 for β_{met} has been shown to describe at best most cosmochemical Mg isotope fractionations since they are kinetic, occurring mostly through evaporation and/or condensation processes.[36-37]

The 2 sigma internal error (2 s.e. or 2σ) on Δ^{26}Mg due to counting statistic errors on the ^{26}Mg/^{24}Mg and ^{25}Mg/^{24}Mg ratios is given by:

$$2\sigma_{(\Delta^{26}Mg)} = \sqrt{(2\sigma_{(\delta^{26}Mg)_{bkgcorr}})^2 + \left(\frac{2}{\beta} \times \sigma_{(\delta^{25}Mg)_{bkgcorr}}\right)^2}.$$

with $\beta = \beta_{Earth}$ or β_{met}, and $\sigma_{(\delta^{25}Mg)_{bkgcorr}}$ and $\sigma_{(\delta^{26}Mg)_{bkgcorr}}$ the errors on the isotope ratios due to counting statistic, typically for an olivine ± 0.014‰ and ± 0.021‰, respectively. To be conservative, the correlation of errors between the $^{26}Mg/^{24}Mg$ and $^{25}Mg/^{24}Mg$ ratios are not taken into account since it could tend to artificially decrease the errors. Note that the relationship between the errors on the isotope ratios and the errors on the delta values is given, for instance for $\delta^{25}Mg$, by:

$$\sigma_{(^{25}Mg/^{24}Mg)} = \frac{0.12663}{10^3} \times \sigma_{(\delta^{25}Mg)}$$

The 2 sigma error on the $\Delta^{26}Mg$ value of an individual measurement $(2\sigma_{(\Delta^{26}Mg)_{ind\text{-}meas}})$ is then calculated as the quadratic sum of (i) the external reproducibility determined from repetitive analyses of standards $(2\sigma_{(\Delta^{26}Mg)_{std}})$ which is of ± 0.010‰ for the session shown in Fig. 2 for example, and (ii) the internal error due to the counting statistic according to:

$$2\sigma_{(\Delta^{26}Mg)_{ind\text{-}meas}} = \sqrt{(2\sigma_{(\Delta^{26}Mg)_{std}})^2 + (2\sigma_{(\delta^{26}Mg)_{bkgcorr}})^2 + \left(\frac{2}{\beta} \times \sigma_{(\delta^{25}Mg)_{bkgcorr}}\right)^2}.$$

When several measurements (n), e.g. different spots in the same object (such as an isolated olivine or a chondrule), give $\Delta^{26}Mg$ values which are identical within ± 2σ then a mean $\Delta^{26}Mg$ value is calculated for this sample as the weighted mean of the n measurements. The 2 sigma error associated with this weighted mean is given by:

$$2\sigma_{(\Delta^{26}Mg)_{weighted-mean}} = 2 \times \sqrt{\frac{1}{\sum_{i=1}^{n} \frac{1}{(\sigma_i^2)_{(\Delta^{26}Mg)_{ind\text{-}meas}}}}}$$

Finally an important comment must be made concerning the differences between the errors on the $\delta^{25}Mg$ and $\delta^{26}Mg$ values and the error on the $\Delta^{26}Mg$ value. Because variations of mass fractionation follow the instrumental fractionation law (in the three Mg isotopes diagram) they do not introduce errors on $\Delta^{26}Mg$. Thus for olivines values of $(2\sigma_{(\Delta^{26}Mg)_{ind\text{-}meas}})$ are typically of 0.06‰ while values of $(2\sigma_{(\delta^{25}Mg)_{ind\text{-}meas}})$or $(2\sigma_{(\delta^{26}Mg)_{ind\text{-}meas}})$ are of 0.20‰ and 0.39‰, respectively, for the session shown in Fig. 2. An interesting application of this observation is that several $\Delta^{26}Mg$ measurements can be made on a small grain (e.g. < 150 μm) successively at the same spot (i.e. by depth profiling). This is a way to improve the precision

on the Δ^{26}Mg value when the grain is too small to make several analyses at different locations. Fig. 3b shows the results of seven such depth profiles made on San Carlos olivines (each depth profile corresponds to five to seven successive analyses). Each depth profile gives Δ^{26}Mg values of 0‰ within their 2 s.e. of typically ± 0.015‰ (the 2 s.d. for each spot varying from 0.028‰ to 0.034‰) despite a significant change of instrumental fractionation with depth in the sample, which results in a range of variation for δ^{25}Mg and δ^{26}Mg values of 0.4‰ and 0.8‰, respectively (Fig. 3a and Table 2).

3.6 Precision reached for the determination of ^{26}Mg excess or deficit

Fig. 4 shows typical results of Δ^{26}Mg measurements for two international and one in-house standards run during one analytical session. The standards show no significant excess or deficit in ^{26}Mg, consistent with their terrestrial origin. The external reproducibility is better than ± 0.04‰ (2 s.d., n=23) and the 2 sigma error on the mean of all analyses of standards is ± 0.018‰ (2 s.e., n=23).

The major source of errors on Δ^{26}Mg values that can be identified in the procedure described here, if an improper treatment of the data is performed, is the correction for instrumental fractionation. Because the instrumental fractionation law is always slightly different from the cosmochemical mass fractionation law and from the terrestrial mass fractionation law, an over-correction or an under-correction of instrumental fractionation (due to a poor calibration of matrix effects) will result in an error on Δ^{26}Mg value (Fig. 5). For instance, correcting for an improper Fo content (e.g Fo#100 instead of Fo#88 for San Carlos olivines) leads to an absolute error on Δ^{26}Mg value of ~ ± 5 ppm. Similarly, using an improper β value (e.g. β_{met} instead of β_{Earth} for San Carlos olivines) can lead to a maximum absolute error of ~ ± 30 ppm on Δ^{26}Mg (Fig. 5 and Table 3).

3.7 Al and Mg relative ion yields

When the ^{26}Mg excesses in meteoritic samples are presumed to be due to the *in situ* decay of short-lived ^{26}Al, isochron diagrams are built to determine the ^{26}Al/^{27}Al ratio at the time of isotopic closure. For that, the ^{27}Al/^{24}Mg ratios must be determined very precisely in order to minimize the error on the ^{26}Al/^{27}Al (e.g. an error of ± 1.3% (see below) in a CAI with ^{26}Al/^{27}Al = 5×10^{-5} introduces an error of ~ ± 1.3% on the ^{26}Al/^{27}Al ratio). Because elemental

secondary ion yields show strong differences between different elements (and different matrices) that cannot be predicted precisely enough from theoretical grounds,[38] they must be calibrated precisely using a set of standards that covers the chemical variability of the samples to analyze.

The Al/Mg relative yield is defined by the ratio between the measured and the true Al/Mg (or $^{27}Al/^{24}Mg$) ratios:

$$\text{Yield}_{(\text{Al/Mg})} = \left(\frac{^{27}\text{Al}}{^{24}\text{Mg}}\right)_{\text{meas}} \Big/ \left(\frac{^{27}\text{Al}}{^{24}\text{Mg}}\right)_{\text{true}}$$

Thus the Al/Mg yield is determined from analyses of international and in-house standards and can then be used to correct measurements of samples. Results of the calibration of the Al/Mg yield for various silicates and oxides are then shown in Table 1. Note that all silicates and oxides such as spinels show (for this analytical session) an averaged Al/Mg yield of 0.77(±0.05, 2 s.d.) with an associated 2 s.e of 1.3% (n=28), while oxides such as hibonites show significantly different yields (0.629(±0.001, 1 s.e.) in this session). Minerals that contain trace amounts of Al, such as olivine, show the same Al/Mg yield than Al-rich silicates within error (1.00(±0.30, 1 s.e.) for olivine from the Eagle Station pallasite, having a Al_2O_3 content of ~ 0.0027 wt%).

The 2 sigma error on the $^{27}Al/^{24}Mg$ ratio is calculated for an individual measurement by summing in a quadratic way the counting error (typically ± 2% (2 s.e.) relative in an olivine and ± 0.2% (2 s.e.) in a mineral like spinel where Al and Mg are major elements) and the two sigma external reproducibility on the standards (typically ± 8% (2 s.e.) in an olivine and ± 1.2% (2 s.e.) in an Al-rich mineral).

4 Examples of the implications of high precision Mg isotopic analyses of components of chondritic meteorites

Using this method, the construction of high precision ^{26}Al isochrons for chondrules and CAIs is within the reach of *in situ* analysis by ion microprobe. Both the slope (from which the initial $(^{26}Al/^{27}Al)_0$ ratio is deduced) and the $(\delta^{26}Mg^*)_0$ intercept (this notation standing for ^{26}Mg excesses or deficits linked to ^{26}Al *in situ* decay) can be precisely determined. This gives theoretically access to the crystallization age (calculated from the $(^{26}Al/^{27}Al)_0$ ratio), and to the ^{26}Al model age of the precursors (calculated from the $(\delta^{26}Mg^*)_0$ value with an appropriate evolution model).

Fig. 6 shows as an example two ^{26}Al isochrons measured for one CAI from the Efremovka CV3 carbonaceous chondrite (data from Mishra and Chaussidon[39]) and for one chondrule from the Semarkona LL3 ordinary chondrite.[8] The CAI isochron has a $(^{26}Al/^{27}Al)_0$ of $4.72(\pm0.10)\times10^{-5}$ and a $(\delta^{26}Mg^*)_0$ of 0.16(±0.06)‰, while the chondrule isochron has a $(^{26}Al/^{27}Al)_0$ of $8.92(\pm0.91)\times10^{-6}$ and a $(\delta^{26}Mg^*)_0$ of -0.0024(±0.0075)‰. If interpreted in a simple model considering that there was a time zero when the inner accretion disk was homogenized to $(^{26}Al/^{27}Al)_i = 5.23\times10^{-5}$ and $(\delta^{26}Mg^*)_i$ = -0.038‰,[5,6,8] the two isochrons imply that the last melting/crystallization event for the CAI and the chondrule took place $0.11^{+0.02}_{-0.02}$ Myr and $1.86^{+0.11}_{-0.10}$ Myr, respectively, after the time zero. A 1.2 to 4 Myr age difference between CAIs and chondrules is a general conclusion of ^{26}Al studies interpreted under the assumption of an homogeneous distribution of ^{26}Al in the inner solar system,[8] which would be consistent with latest accretion models considering progressive gravitational collapse of mm-sized particles concentrated by turbulence in the nebular gas (see review by Dauphas and Chaussidon[40]).

The different $(\delta^{26}Mg^*)_0$ observed for the CAI and the chondrule can be understood as reflecting different origins and histories for their precursors. The simplest model would be for the chondrule that the precursors were condensed from the nebular gas at 1.86 Myr (age given by the $(^{26}Al/^{27}Al)_0$ of the chondrule isochron): ^{26}Al decay in the nebular gas with a $^{27}Al/^{24}Mg$ of 0.101 for 1.86 Myr would result in a $\delta^{26}Mg^*$ of -0.007‰. For the CAI, the simplest model is that its precursors were condensed at time zero and then evolved in closed system with the bulk $^{27}Al/^{24}Mg$ ratio of the CAI of 7.10, leading to the build up of a $\delta^{26}Mg^*$ of 0.16‰ in 0.08 Myr. However more complicated scenarios are possible[13,35] depending on the model considered.

High precision Mg-isotope measurements are also possible for Mg-rich and Al-poor phases (i.e. phases with a low Al/Mg ratio). This is the case for Mg-rich refractory olivines (either isolated olivines or olivines in porphyritic type I chondrules), whose ^{26}Al model ages could be constrained. These Mg-rich olivines may have various origins. Because they are virtually devoid of Al no radiogenic in-growth of ^{26}Mg takes place, so that their Mg isotopic composition will reflect that of their source, i.e. the nebular gas from which they condensed, the chondrule melt from which they crystallized,[41-43] or the planetesimal mantle from which they crystallized.[44-48] For a given model, the precision on the ^{26}Al model age calculations of these Mg-rich refractory olivines is highly dependent on the precision on both the Δ^{26}Mg value and the $^{27}Al/^{24}Mg$ ratio. For instance for a parent melt with a $^{27}Al/^{24}Mg$ ratio of 2.5, a

precision of ± 0.016‰ on $\Delta^{26}Mg$ leads to a precision on the age of ± 0.02 Ma (data from Luu *et al.*[49]).

5 Conclusion

The analytical protocol and data reduction process described in this study allow high precision to be reached for Mg isotopic measurements ($^{25}Mg/^{24}Mg$ and $^{26}Mg/^{24}Mg$ ratios, as well as ^{26}Mg excess) by MC-SIMS. This method minimizes analytical bias on the final Mg-isotope results, that is very important at the level of precision targeted in cosmochemistry (better than 10 ppm absolute error on the calculation of the final ^{26}Mg excess or deficit).
This new possibility of reaching very high precision for Mg-isotope analyses opens new perspectives in geo- and cosmochemisty fields. For instance natural processes such as biomineralization could be better understood by more accurately constraining the induced fractionation.

6 Acknowledgements

This work was supported by grant from European Research Council (ERC grant FP7/2007-2013 Grant Agreement no. [226846] Cosmochemical Exploration of the first two Million Years of the Solar System — CEMYSS).

7 References

1 A. Bouvier and M. Wadhwa, *Nature Geoscience*, 2010, **3**, 637–641.

2 Y. Amelin, A. N. Krot, I. D. Hutcheon and A. A. Ulyano, *Science*, 2002, **297**, 1678–1683.

3 J. Connelly, Y. Amelin, A. N. Krot and M. Bizzarro, *Astrophys. J.*, 2008, **675**, L121-L124.

4 T. Lee, D. A. Papanastassiou and G. J. Wasserburg, *Geophys. Res. Lett.*, 1976, **3**, 109-112.

5 K. Thrane, M. Bizzarro and J. A. Baker, *Astrophys. J.*, 2006, **646**, L159-L162.

6 B. Jacobsen, Q. Z. Yin, F. Moynier, Y. Amelin, A. N. Krot, K. Nagashima, I. D. Hutcheon and H. Palme, *Earth Planet. Sci. Lett.*, 2008, **272**, 353-364.

7 K. Lodders, *Astrophys. J.,* 2003**, 591**, 1220-1247.

8 J. Villeneuve, M. Chaussidon and G. Libourel, *Science*, 2009, **325**, 985-988.

9 K. K. Larsen, A. Trinquier, C. Paton, M. Schiller, D. Wielandt, M. A. Ivanova, J. N. Connelly, A. Nordlund, A. N. Krot and M. Bizzarro, *Astrophys. J.,* 2011,**735**, L37.

10 M. Bizzarro, C. Paton, K. Larsen, M. Schiller, A. Trinquier and D. Ulfbeck, *J. Anal. At. Spectrom.*, 2011, **26**, 565-577.

11 J. Villeneuve, M. Chaussidon and G. Libourel, *Earth Planet. Sci. Lett.*, 2011, **301**, 107-116.

12 G. J. MacPherson, E. S. Bullock, P. E. Janney, N. T. Kita, T. Ushikubo, A. M. Davis, M. Wadhwa and A. N. Krot, *Astrophys. J.,* 2010**, 711**, L117-L121.

13 G. J. MacPherson, N. T. Kita, T. Ushikubo, E. S. Bullock and A. M. Davis, *Earth Planet. Sci. Lett.*, 2012, **331-332**, 43-54.

14 N. T. Kita and T. Ushikubo, *Meteoritics*, in press, doi:10.1111/j.1945-5100.2011.01264.x.

15 N. T. Kita, T. Ushikubo, K. B. Knight, R. A. Mendybaev, A. M. Davis, F. M. Richter and J. H. Fournelle, *Geochim. Cosmochim. Acta*, in press, doi:10.1016/j.gca.2012.02.015.

16 A. Benninghoven, F. G. Rüdenauer, and H. W. Werner, Secondary Ion Mass Spectrometry: Basic Concepts, Instrumental Aspects, Applications, and Trends, eds. Wiley, New York, 1987, 1227 pages.

17 E. de Chambost, F. Hillion, B. Rasser, H. N. Migeon, in SIMS VIII Proceedings, eds. A. Benninghoven, K. T. F. Janssen, J. Tumpner, H. W. Werner, New York: John Wiley, 1991, pp. 207-210.

18 E. J. Catanzaro, T. J. Murphy, E. L. Garner and W. R. Shields, *J. Res. Natl. Bur. Stand.*, 1966, **70A**, 453-458.

19 R. C. Ogliore, G. R. Huss and K. Nagashima, *Nucl.Instrum. Methods Phys. Res. B*, 2011, **269**, 1910-1918.

20 E. De Chambost 1997, User's Guide for Multicollector Cameca IMS 1270. Cameca, Courbevoie, France.

21 D. A. Ionov, I. V. Ashchepkov, H.-G. Stosch, G. Witt-Eickschen and H. A. Seck, *J. Petrology,* 1993, **34**, 1141-1175.

22 S. Decitre 2000, PhD thesis, Centre de Recherches Pétrographiques et Géochimiques (CRPG-CNRS), Nancy.

23 S. Gao, X. Liu, H. Yuan, B. Hattendorf, D. Günther, L. Chen and S. Hu, *Geostand. Newsletter*, 2002, **26**, 181-196.

24 W. Yang, F.-Z. Teng and H.-F. Zhang, *Earth Planet. Sci. Lett.*, 2009, **288**, 475-482.

25 F.-Z. Teng, W.-Y. Li, S. Ke, B. Marty, N. Dauphas, S. Huang, F.-Y. Wu and A. Pourmand, *Geochim. Cosmochim. Acta*, 2010, **74**, 4150–4166.

26 E. Deloule, C. France-Lanord and F. Albarède, in Stable isotope geochemistry: a tribute to Samuel Epstein, eds. H. P. Taylor, Jr., J. R. O'Neil and I. R. Kaplan, 1991, pp. 53-62.

27 E. D. Young and A. Galy, *Rev. Min. Geochem.*, 2004, **55**, 197-230.

28 K. R. Ludwig, ISOPLOT 3: A geochronological toolkit for microsoft excel, Berkeley Geochronology Centre Special Publication, 4, 2003, 74pp.

29 F. Albarède and B. Beard, *Rev. Min. Geochem.*, 2004, **55**, 113-152.

30 L. A. Leshin, A. E. Rubin and K. D. McKeegan, *Geochim. Cosmochim. Acta*, 1997, **61**, 835–845.

31 A. Galy, N. S. Belshaw, L. Halicz and R. K. O'Nions, *Int. J. Mass Spectrom.*, 2001, **208**, 89-98.

32 E. B. Boulou-Bi, N. Vigier, A. Brenot and A. Poszwa, *Geostand. Geoanal. Res.,* 2009*,* **33**, 95-109.

33 A. Galy, O. Yoffe, P. E. Janney, R. W. Williams, C. Cloquet, O. Alard, L. Halicz, M. Wadhwa, I. D. Hutcheon, E. Ramon and J. Carignan, *J. Anal. At. Spectrom.*, 2003, **18**, 1352-1356.

34 E. D. Young, A. Galy and H. Nagahara, *Geochim. Cosmochim. Acta*, 2002, **66**, 1095-1104.

35 A. M. Davis, F. M. Richter, R. A. Mendybaev, P. E. Janney, M. Wadhwa and K. D. McKeegan, *36th Lunar Planet. Inst. Conf.*, League City, Texas, 2005.

36 A. M. Davis, A. Hashimoto, R. N. Clayton and T. K. Mayeda, *Nature*, 1990, **347**, 655–658.

37 A. M. Davis and F. M. Richter, in Treatise on Geochemistry, Vol. 1: Meteorites, Planets, and Comets, ed. A. M. Davis, eds. H. D. Holland and K. K. Turekian, Oxford: Elsevier-Pergamon, 2003, pp. 407-430.

38 R. W. Hinton, *Chem. Geol.*, 1990, **83**, 11-25.

39 R. K. Mishra and M. Chaussidon, *43rd Lunar Planet. Sc. Conf.*, Texas, 2012.

40 N. Dauphas and M. Chaussidon, *Annu. Rev. Earth Planet. Sci.*, 2011, **39**, 351-386.

41 N. G. Rudraswami, T. Ushikubo, D. Nakashima and N. T. Kita, *Geochim. Cosmochim. Acta*, 2011, **75**, 7596-7611.

42 H. Nagahara, *Nature,* 1981**, 292**, 135-136.

43 R. H. Jones, in International conference: Chondrules and the protoplanetary disk, eds. R. H. Hewins, R. H. Jones and E. R. D. Scott, Cambridge University Press, 1996, pp. 163-172.

44 L. Tissandier, G. Libourel and F. Robert, *Meteoritics*, 2002, **37**, 1377-1389.

45 G. Libourel, A. N. Krot and L. Tissandier, *Earth Planet. Sci. Lett.*, 2006, **251**, 232-240.

46 G. Libourel and A. N. Krot, *Earth Planet. Sci. Lett.*, 2007, **254**, 1-8.

47 M. Chaussidon, G. Libourel and A. N. Krot, *Geochim. Cosmochim. Acta*, 2008, **72**, 1924-1938.

48 G. Libourel and M. Chaussidon, *Earth Planet. Sci. Lett.*, 2011, **301**, 9-21.

49 T.-H. Luu, M. Chaussidon and J.-L. Birck, *43rd Lunar Planet. Sc. Conf.*, Texas, 2012.

Tables

Table 1: Chemical composition for some major elements, and Al/Mg yield, of the terrestrial reference materials and international standards used in this study.

Standards	SiO_2 * (wt%)	Al_2O_3 * (wt%)	MgO * (wt%)	$^{27}Al/^{24}Mg$ * (atomic)	$^{27}Al/^{24}Mg$ ** (ion microprobe)	Al/Mg yield
San Carlos olivine [1]	40.33	0.03	48.87	6.14×10^{-4}	4.67×10^{-4}	0.76
Eagle Station (MNHN) olivine [1]	39.29	2.72×10^{-3}	42.69	6.37×10^{-5}	6.36×10^{-5}	1.00[a]
Clinopyroxene BZCG (Zabargad) [2]	50.35	7.05	14.11	0.50	0.38	0.76
Clinopyroxene BZ 226 (Zabargad) [2]	51.36	4.49	15.35	0.29	0.23	0.80
Clinopyroxene 313-3 (Vitim) [3]	52.84	5.81	15.52	0.37	0.28	0.75
Orthopyroxene BZ 226 (Zabargad) [2]	54.14	3.85	31.20	0.12	0.10	0.78
Orthopyroxene 313-3 (Vitim) [3]	55.16	3.73	32.94	0.11	0.09	0.77
Spinel (Burma) [1]	0.02	71.66	27.88	2.57	1.86	0.72
Spinel 86-1 (Vitim) [3]	0.06	57.33	20.9	2.75	2.07	0.75
Basaltic glass MORB CLDR015V [1]	50.43	15.83	8.43	1.88	1.41	0.75
Basaltic glass BHVO (Hawaii) [1]	49.90	13.50	7.23	1.87	1.41	0.75
Basaltic glass BCR2 (Columbia river) [1]	54.10	13.50	3.59	3.76	2.97	0.79
Synthetic anorthitic glass [1]	44.05	34.66	1.79	19.41	14.83	0.76
Synthetic melilitic glass [1]	41.00	11.00	7.00	1.57	1.10	0.70
Synthetic pyroxenic glass [1]	44.38	14.78	11.21	1.32	1.04	0.79
Synthetic glass Bacati [1]	31.01	30.74	10.29	2.99	2.41	0.81
Synthetic glass Al20 [1]	48.68	20.09	9.52	2.11	1.66	0.79
Synthetic glass Al10 [1]	55.05	10.41	11.37	0.92	0.74	0.81
Synthetic glass Al5 [1]	58.31	5.11	11.17	0.46	0.38	0.83
Synthetic glass NIST SRM 614 [4]	71.83	2.29	0.01	435.85	336.90	0.77
Synthetic glass NIST SRM 610 [4]	69.06	2.20	0.08	28.84	21.82	0.76
Hibonite (Madagascar) [1]	0.88	73.70	2.91	25.35	15.95	0.63

[1,2,3,4] stand for chemical composition data coming from this study, Decitre (2000), Ionov *et al.* (1993) and Gao *et al.* (2002), respectively.

* indicates that the 1 sigma error is typically ± 2% for SiO_2, Al_2O_3 and MgO analyses and for the resulting $(^{27}Al/^{24}Mg)_{atomic}$ ratio.

** indicates that the 1 sigma error is typically better than ± 1.5% for $(^{27}Al/^{24}Mg)_{ion\ microprobe}$ measurements

[a] the 1 sigma error on the Al/Mg yield of Eagle Station olivine is ± 0.30.

Table 2: Mg isotopic compositions of olivines from the San Carlos terrestrial reference material (Fo#88).

Name	Description	δ^{25}Mg (‰)	2 s.e	δ^{26}Mg (‰)	2 s.e	Δ^{26}Mg (‰)	2 s.e	n
SC 1	separated grain	- 0.180	0.103	- 0.343	0.206	0.017	0.020	10
SC 2	separated grain	- 0.058	0.059	- 0.118	0.126	- 0.006	0.023	7
average						*0.007*	*0.015*	*17*
SC P1	separated grain - profile n°1	- 0.514	0.029	- 0.912	0.067	- 0.007	0.012	6
SC P2	separated grain - profile n°2	- 0.522	0.032	- 0.939	0.078	- 0.015	0.012	6
SC P3	separated grain - profile n°3	- 0.493	0.049	- 0.862	0.092	0.002	0.014	6
SC P4	separated grain - profile n°4	- 0.346	0.025	- 0.582	0.043	0.004	0.012	5
SC P5	separated grain - profile n°5	- 0.379	0.024	- 0.631	0.035	0.015	0.013	6
SC P6	separated grain - profile n°6	- 0.552	0.026	- 0.969	0.048	0.013	0.012	7
SC P7	separated grain - profile n°7	- 0.694	0.042	- 1.263	0.079	- 0.011	0.014	6
average						*0.003*	*0.005*	*42*
Average						**0.002**	**0.009**	

Table 3: Effect on the instrumental fractionation of an improper matrix effect correction on San Carlos olivines (Fo#88). The use of an improper Fo content and/or an improper β (β_{Earth} or β_{met}) value both impacts the final Δ^{26}Mg value (see text). The 2 s.e. on Δ^{26}Mg values is ± 0.024‰ whatever the case. Fo# =MgO/(FeO+MgO) (wt%/wt%).

	δ^{25}Mg (‰)	Δ^{26}Mg (‰)	
		β_{Earth} = 0.521	β_{met} = 0.514
Fo#79	-0.997	-0.010	0.016
Fo#88	-0.058	-0.006	-0.004
Fo#100	1.199	-0.001	-0.031

Figure captions

1) The correction for drifts of Faraday cup backgrounds using a linear interpolation between two successive analyses impacts both δ^{25}Mg (black dots) and δ^{26}Mg values (not shown), with a more important effect on Mg-poor minerals (spinel, pyroxene) compared to Mg-rich minerals (olivines for instance). The background correction also affects Δ^{26}Mg values (open squares): this non-mass dependent correction is due to lower count rates on ^{25}Mg and ^{26}Mg compared to ^{24}Mg, with a maximum of 10 ppm change for olivines for instance.
2) Example of a Mg isotopic instrumental fractionation law, calibrated using reference materials with different compositions (San Carlos olivine, Burma spinel and synthetic pyroxene). Slope and intercept are calculated using the Isoplot 3.00 software.[28] Large variations of $\ln(\alpha_{inst}^{25/24})$ values are present among silicates and oxides, and are linked to matrix effects which result from variations of vibrational energies of the bonds involving Mg isotopes in minerals or glasses having different chemical compositions.
3) Mg isotopic compositions of San Carlos olivines (Fo#88) measured using two different protocols: either single measurements at different spots (black (SC1) and open (SC2) diamonds, corresponding to two different separated San Carlos olivine grains) or depth profiles (black dots). All data are corrected for matrix effect. The true Mg-isotope composition of San Carlos olivines is also plotted (open star). a) Three Mg-isotope diagram showing that the two types of data follow the same fractionation law (even if the fractionation is in average stronger for depth profiles). Error bars, typically better than ± 0.11‰ on δ^{25}Mg values and ± 0.22‰ on δ^{26}Mg values for this analytical session, are not shown for simplicity. b) Averages of analyses made by depth profiles at different spots (n is the number of analyses in a given depth profile, black dots) compared to the average of the single analyses (n=10) made at different spots (open diamond). Both types of measurements show Δ^{26}Mg values correctly determined at 0‰ within 2 s.e. Thus, depth profiles can be used in small samples to obtain a precision on Δ^{26}Mg values similar to that obtained from averaging several analyses made at different locations.
4) ^{26}Mg excess or deficit (expressed with the Δ^{26}Mg notation, see text) obtained for three reference materials with different chemical compositions (the same as in Fig. 2) measured within one analytical session (n=23). They show no significant excess or deficit in ^{26}Mg, consistent with their terrestrial origin. The typical external reproducibility (2 s.d.) is better than ± 0.04‰ while the 2 sigma error of each individual measurement is typically better

than ± 0.06‰. The 2 sigma error on the mean of all analyses of reference materials (2 s.e.) is better than ± 0.02‰.

5) Schematic effect in a three Mg isotope diagram of an improper correction for instrumental isotopic fractionation on the determination of the Δ^{26}Mg value of meteoritic samples. The open dot stands for the isotopic composition after appropriate corrections (see text). In this example no ^{26}Mg excess is obtained since the open dot is sitting on the cosmochemical fractionation line (see text). The two black dots represent wrong corrections of instrumental fractionation in which matrix effect was under- or over-estimated: this results in "wrong" apparent ^{26}Mg excess or deficit relative to the cosmochemical line (dark grey field). Using erroneously the terrestrial line instead of the cosmochemical line also results in "wrong" ^{26}Mg excess or deficit (light grey field).

6) Two ^{26}Al isochrons measured for one CAI from the Efremovka CV3 carbonaceous chondrite (MSWD = 1.15, data from Mishra and Chaussidon, 2012) and for one chondrule from the Semarkona LL3 ordinary chondrite (MSWD = 0.71, data from Villeneuve *et al.*, 2009). A gap ranging from 1.2 to 4 Myr between the ^{26}Al ages of CAIs and chondrules is generally deduced from ^{26}Al studies assuming a homogeneous distribution of ^{26}Al and Mg isotopes in the accretion disk.

Figures

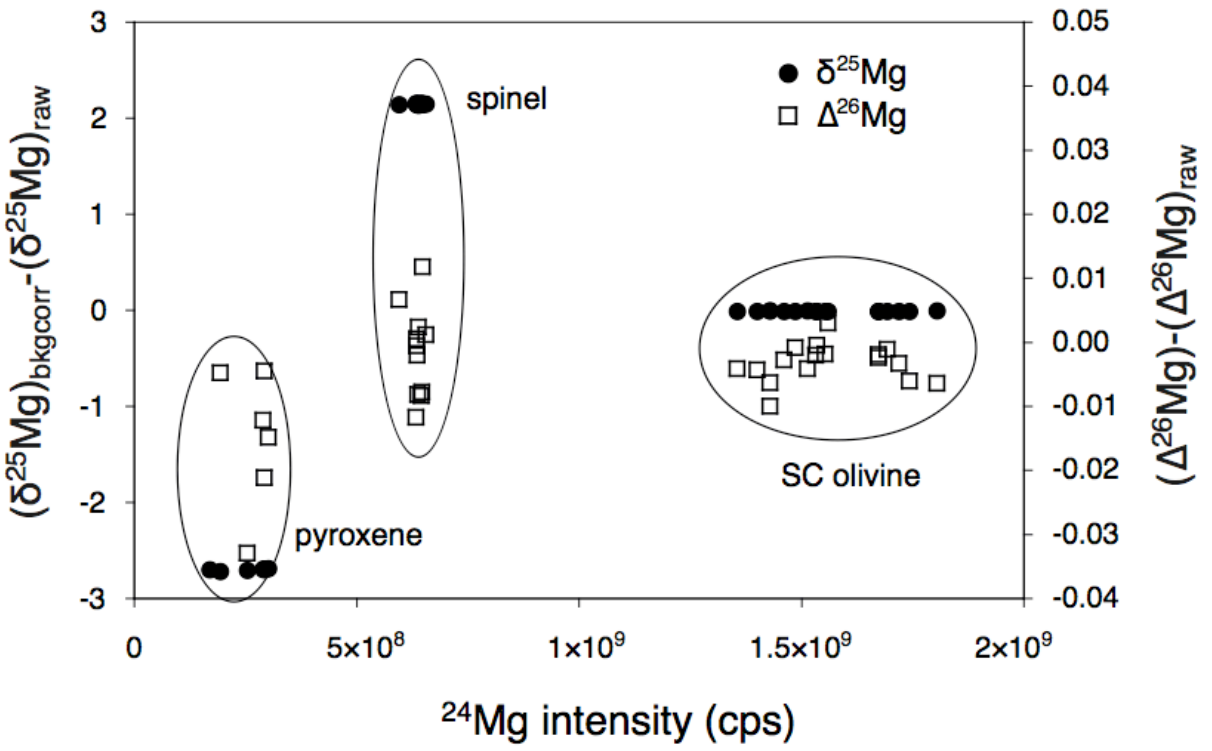

FIGURE 1

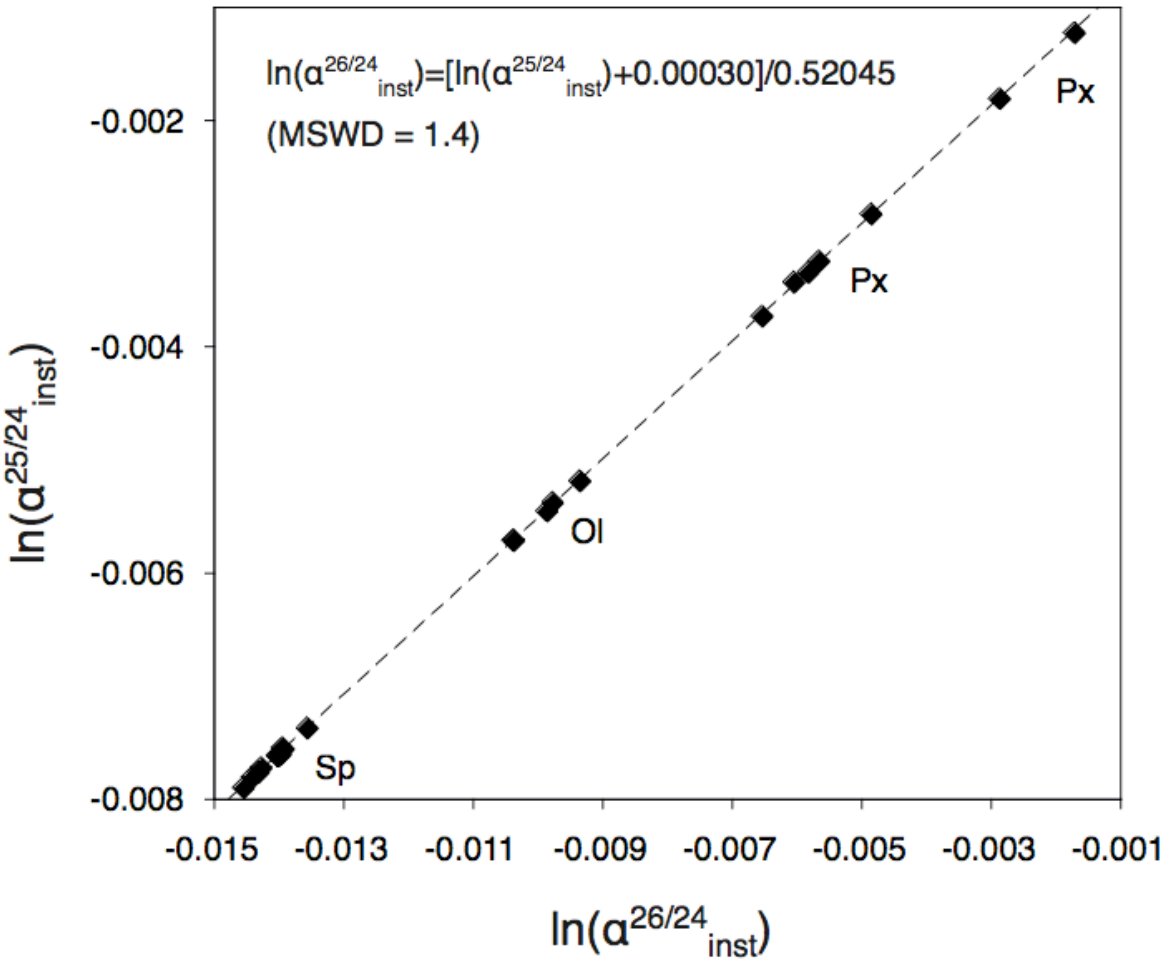
ln(α26/24inst)=[ln(α25/24inst)+0.00030]/0.52045
(MSWD = 1.4)
Px
Px
Ol
Sp
-0.002
-0.004
-0.006
-0.008
-0.015
-0.013
-0.011
-0.009
-0.007
-0.005
-0.003
-0.001
ln(α25/24inst)
ln(α26/24inst)

FIGURE 2

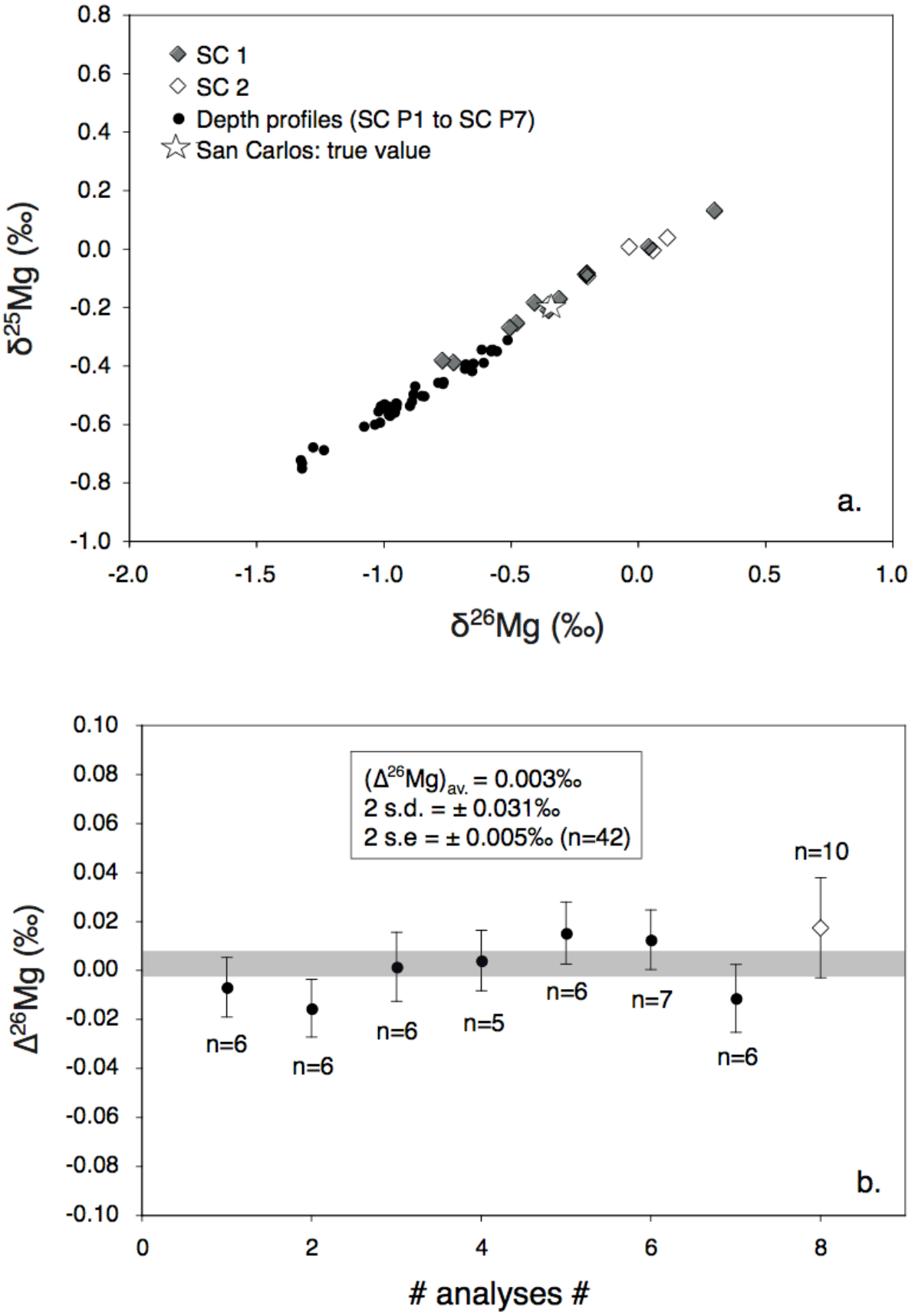
SC 1
SC 2
Depth profiles (SC P1 to SC P7)
San Carlos: true value
a.
δ25Mg (‰)
δ26Mg (‰)
(Δ26Mg)av. = 0.003‰
2 s.d. = ± 0.031‰
2 s.e = ± 0.005‰ (n=42)
n=6
n=6
n=6
n=5
n=6
n=7
n=6
n=10
b.
Δ26Mg (‰)
analyses

FIGURE 3

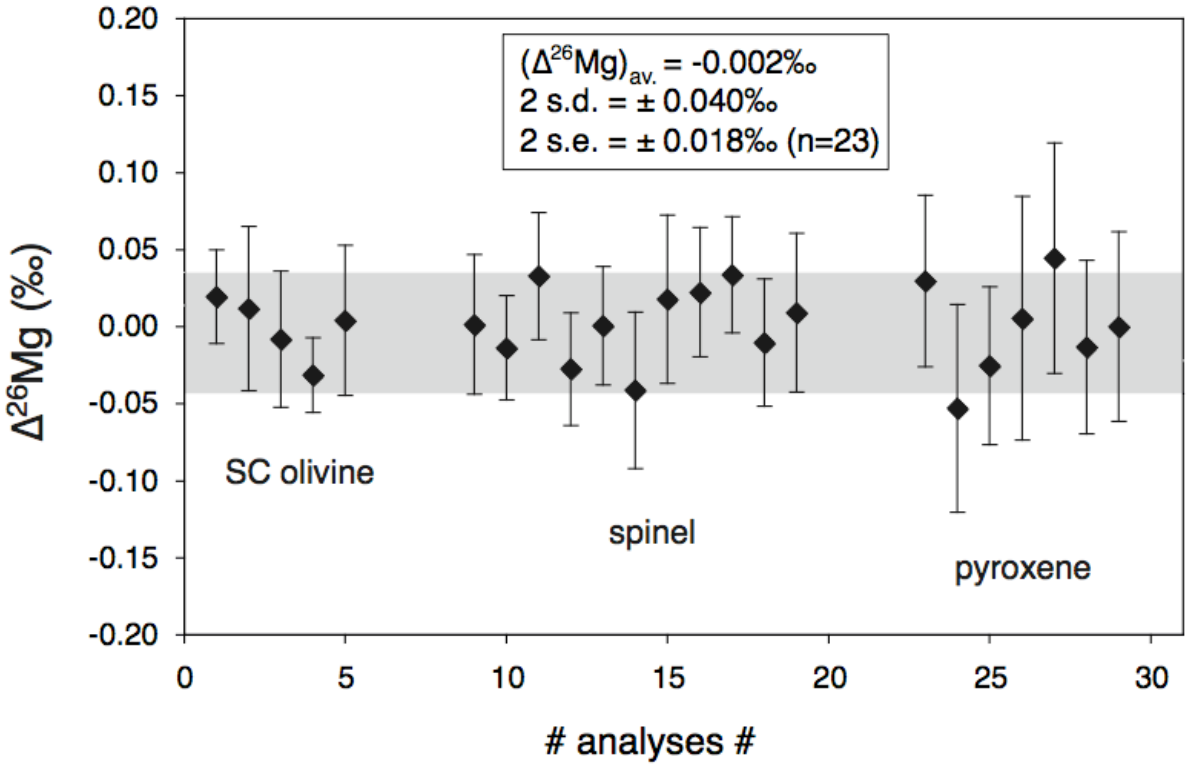
$(\Delta^{26}Mg)_{av.}$ = -0.002‰
2 s.d. = ± 0.040‰
2 s.e. = ± 0.018‰ (n=23)
SC olivine
spinel
pyroxene
$\Delta^{26}Mg$ (‰)
analyses
0.20
0.15
0.10
0.05
0.00
-0.05
-0.10
-0.15
-0.20
0
5
10
15
20
25
30

FIGURE 4

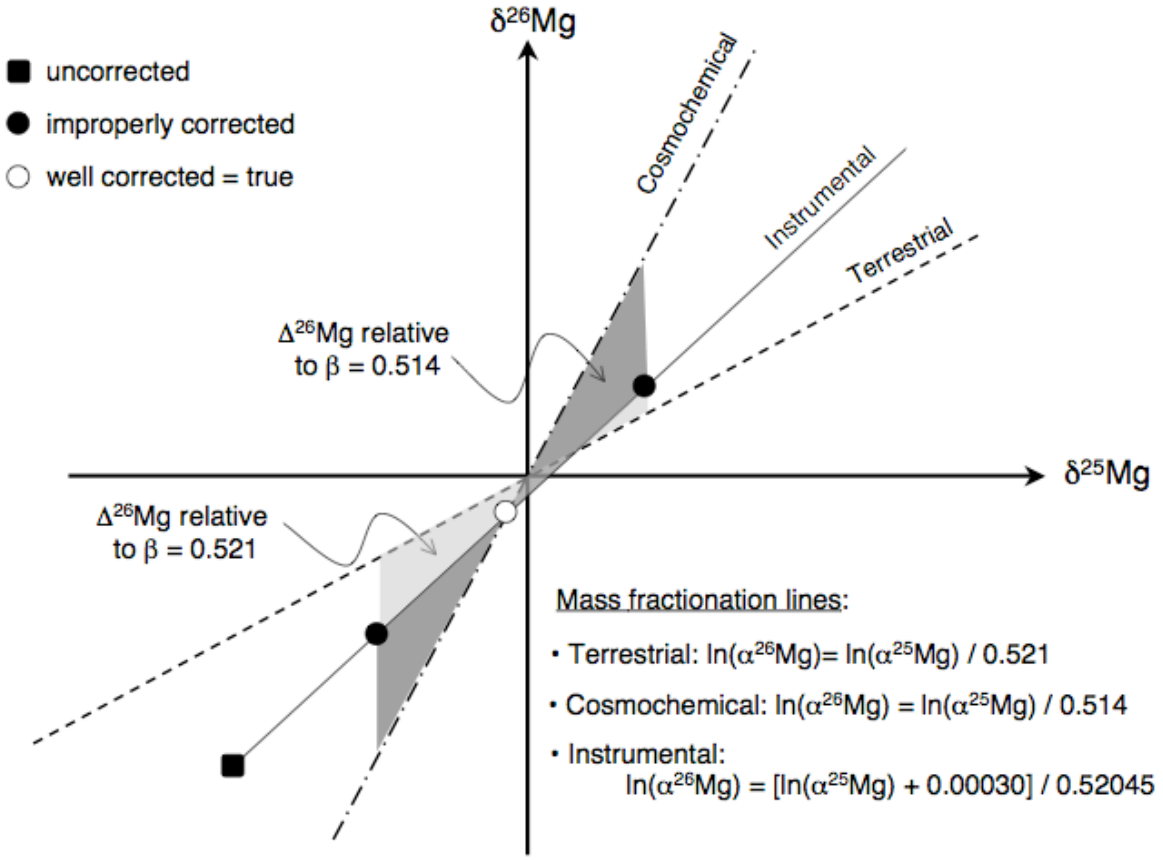
uncorrected
improperly corrected
well corrected = true
δ26Mg
Cosmochemical
Instrumental
Terrestrial
Δ26Mg relative to β = 0.514
δ25Mg
Δ26Mg relative to β = 0.521
Mass fractionation lines:
• Terrestrial: ln(α26Mg)= ln(α25Mg) / 0.521
• Cosmochemical: ln(α26Mg) = ln(α25Mg) / 0.514
• Instrumental:
ln(α26Mg) = [ln(α25Mg) + 0.00030] / 0.52045

FIGURE 5

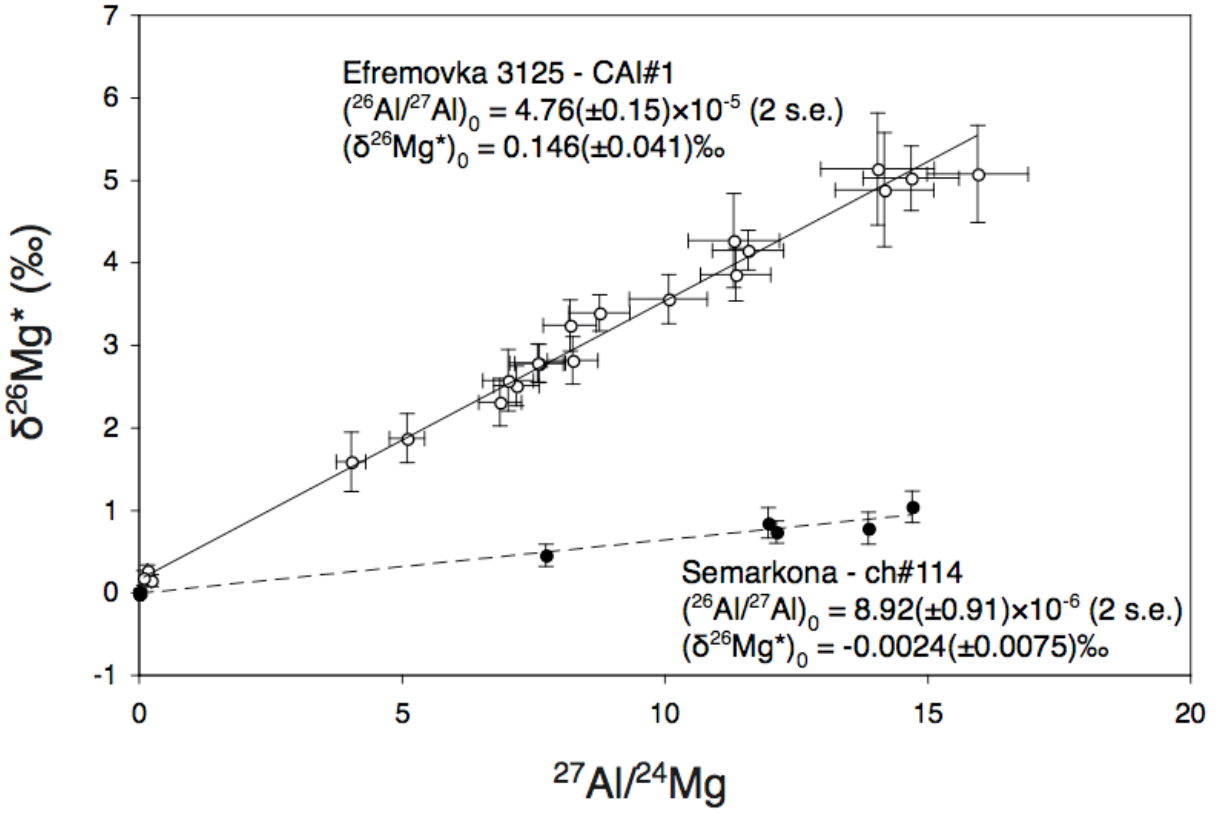
Efremovka 3125 - CAI#1
$(^{26}Al/^{27}Al)_0 = 4.76(\pm0.15)\times10^{-5}$ (2 s.e.)
$(\delta^{26}Mg^*)_0 = 0.146(\pm0.041)‰$
Semarkona - ch#114
$(^{26}Al/^{27}Al)_0 = 8.92(\pm0.91)\times10^{-6}$ (2 s.e.)
$(\delta^{26}Mg^*)_0 = -0.0024(\pm0.0075)‰$
$\delta^{26}Mg^*$ (‰)
$^{27}Al/^{24}Mg$
7
6
5
4
3
2
1
0
-1
0
5
10
15
20

FIGURE 6